Exchange of optical vortices in symmetry-broken quantum systems

Seyyed Hossein Asadpour,[1,*] Emmanuel Paspalakis,[2,†] and Hamid R. Hamedi[3,‡]
[1]*School of Physics, Iran University of Science and Technology, Tehran 1684613114, Iran*
[2]*Materials Science Department, School of Natural Sciences, University of Patras, Patras 265 04, Greece*
[3]*Institute of Theoretical Physics and Astronomy, Vilnius University, Saulėtekio 3, Vilnius LT-10257, Lithuania*

(Received 29 January 2021; accepted 24 May 2021; published 7 June 2021)

We investigate the interaction of laser pulses carrying orbital angular momentum (OAM) with a symmetry-broken ladder-type quantum coupling scheme involving three internal states. A weak probe beam acts on the lower leg of the ladder scheme, while a control beam of higher intensity drives the upper leg. In contrast to natural atoms, such a model with broken symmetry allows generating a sum-frequency signal beam between the most upper and lower quantum states, forming a cyclic closed-loop configuration of light-matter interaction. We propose situations for the efficient transfer of optical vortices to the generated signal beam via a nonlinear three-wave mixing process. It is demonstrated that the exchange process can occur both in the electromagnetically induced transparency (EIT) and the Autler-Townes splitting (ATS) regimes. The transition between the EIT and ATS conversion schemes can smoothly happen by simply tuning the knob of the control field. It is shown that the ATS regime is considerably more favorable than the EIT to achieve maximum energy conversion efficiency between light beams carrying the OAM. The results may provide an applications-based perspective to the ongoing research centered on vortex conversion-based comparisons between the ATS and EIT.

DOI: 10.1103/PhysRevA.103.063705

I. INTRODUCTION

Electromagnetically induced transparency (EIT) [1–4] is a quantum interference effect which appears when coherent laser beams interplay with an atomic system. The quantum interference in EIT occurs between alternative transition channels induced by the laser beams within the internal states of the atom. As a result, in the EIT the absorption effects are suppressed for a weak resonant probe field for which strong absorption would normally be expected [4]. EIT has a number of interesting applications, such as enhanced four-wave-mixing [5–8], lasing without inversion [9], slow and fast light [10–13], enhancement of refractive index [14,15], ultraslow optical solitons [16–18], large optical Kerr nonlinearity [19–21], and many others.

The quantum interference responsible for the EIT vanishes for strong laser fields, resulting in the Autler-Townes splitting (ATS) effect [22,23]. The EIT and ATS schemes resemble each other in terms of a transparency feature, but they are essentially different quantum optical phenomena. The EIT stems from a Fano-type interference and is described by the formation of a dark-state due to a destructive quantum interference between different transition pathways [4], whereas ATS is described by the AC-Stark effect [23]. Distinctions between EIT and ATS have been widely studied and discussed in the literature [24–32].

Optical vortex beams [33,34] are of fundamental interest due to their applications. An optical vortex with a spiral phase carries an orbital angular momentum (OAM) along the propagation axis [33]. There is a phase singularity at the core of the vortex which evolves its doughnut-shaped intensity profile. Optical vortices are routinely created to carry specific values of OAM [35,36]. When interacting with the matter, their specific characteristics result in various interesting effects, including ultraprecise atom localization [37], entanglement of OAM states of photon pairs [38], atom vortex beams [39], light-induced torque [40–42], and spatially dependent EIT [43,44].

A transition from a nontrivial (vortex) to a trivial (non-vortex) state of the light is very promising and may provide interesting applications in the topological photonic area. The exchange of optical vortices is a possible tool for the manipulation of information encoded into the OAM of light [45]. It allows generating a structured light at a wavelength for which it is not possible to do it directly with standard optics (e.g., far infrared or UV). Although the exchange of optical vortices is not directly related to the topological photonics, optical vortices can be used for creating the synthetic gauge field for ultracold atoms [46].

In this context, the recently proposed and demonstrated protocols for exchange of optical vortices in mater waves have emerged as a direct connection to the OAM-based applications. Previous scenarios for the OAM translation have been shown to be possible in the regime of EIT (or Coherent population trapping) [47–55]. However, ATS has not gained nearly as much attention. This oversight may be partly because of a common misconception that quantum interference is a necessary characteristic for an efficient OAM exchange, and partly due to lack of interest in the ATS regime.

Extending previous work, in this study we make a detailed comparison between the EIT and ATS protocols in order to

*s.hosein.asadpour@gmail.com
†paspalak@upatras.gr
‡Hamid.hamedi@tfai.vu.lt

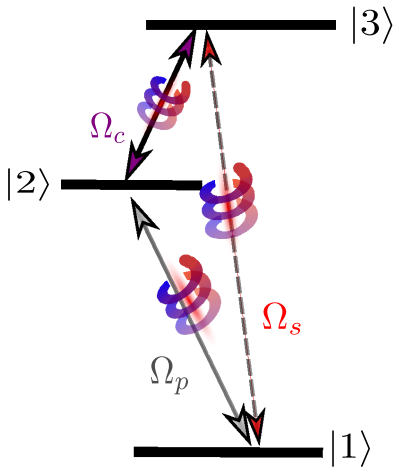

FIG. 1. Interaction of a symmetry-broken three-level ladder quantum system with three laser beams which can carry optical vortices.

achieve an efficient transfer of optical vortices in a three-level ladder-type quantum coupling scheme. The ladder-type quantum system has been widely used for appearance of EIT and ATS [56,57]. The system involves a weak probe field as well as a strong control field which are interacting with lower and upper legs of the ladder, respectively. As a result of inversion symmetry of potential energy in natural atoms, the sum-frequency process is forbidden in the ladder scheme. However, the common electric-dipole selection rules do not matter when the inversion symmetry of potential energy in a quantum system is broken. This leads to generation of a three-wave mixing (TWM) signal beam between the upper and lower quantum states of the ladder scheme, creating a cyclic closed-loop configuration of light-matter interaction [58–64]. Note that the ladder-type quantum system considered here has been recently employed for the purpose of efficient nonlinear frequency mixing [64]. However, the interplay of such a quantum system with laser pulses carrying optical vortices has motivated our study. We propose situations for efficient exchange of OAM beams between different frequencies via a nonlinear TWM process. The control field intensity plays a critical role for a smooth transition between the EIT and ATS schemes for the signal beam. We compare both EIT and ATS protocols for exchange of vortices, and find that the ATS provides a more favorable scenario than EIT in order to achieve high conversion efficiency.

II. MODEL AND FORMULATION

We consider a quantum system characterized by a three-level ladder scheme of energy levels, shown in Fig. 1. The scheme involves a ground level $|1\rangle$ and two excited states $|2\rangle$ and $|3\rangle$. The quantum system interacts with a probe field of lower intensity (with the frequency ω_p, wave vector k_p) coupling the transition $|1\rangle \leftrightarrow |2\rangle$, and a control field of much higher intensity (with the frequency ω_c, wave vector k_c) coupling the transition $|2\rangle \leftrightarrow |3\rangle$. The channel $|1\rangle \leftrightarrow |3\rangle$ is usually forbidden in natural atoms due to presence of selection rules which prevent any three-wave mixing. However, this transition is allowed in the symmetry-broken quantum systems, leading to a second-order nonlinear mixing signal with a new frequency $\omega_s = \omega_p + \omega_c$. The nonlinear process for sum-frequency generation can be described with the phase-matching condition $k_s = k_p + k_c$.

Applying the rotating-wave approximation for such a quantum system, the interaction Hamiltonian reads ($\hbar = 1$)

$$H = \delta_p\sigma_{22} + \delta_p\sigma_{33} - \tfrac{1}{2}(\Omega_p\sigma_{21} + \Omega_c\sigma_{32} + \Omega_s\sigma_{31} + \text{H.c.}), \tag{1}$$

where $\delta_p = \omega_{21} - \omega_p$ is the detuning of the probe field, Ω_p, Ω_c and Ω_s characterize the probe, control, and signal laser fields, respectively, defined by $\Omega_p = \mu_{12}E_p/\hbar$, $\Omega_s = \mu_{13}E_s/\hbar$, $\Omega_c = \mu_{23}E_c/\hbar$, where μ_{ij} is the electric dipole matrix element associated with the transition from $|i\rangle$ to $|j\rangle$, and E_p, E_c, E_s are the slowly varying amplitudes of the applied fields. Moreover, $\sigma_{ij} = |i\rangle\langle j|$ characterizes the projection operator of the ladder quantum scheme.

The control field frequency ω_c is considered to match the energy spacing ω_{32} between the levels $|2\rangle$ and $|3\rangle$. Yet, there is one more detuning condition which should be satisfied ($\delta_s = \delta_p + \delta_c$), leading to the energy requirement condition $\omega_s = \omega_p + \omega_c$. Since we assume $\delta_c = 0$, this leads to $\delta_s = \delta_p$, which has been applied in the Hamiltonian of Eq. (1). This implies that the change in one detuning will also change the other one.

The equations of the motion for the matter fields are

$$\begin{aligned}
\dot\rho_{31} &= (\gamma_{31} + i\delta_p)\rho_{31} + \frac{i}{2}\Omega_s(\rho_{11} - \rho_{33}) + \frac{i}{2}\Omega_c\rho_{21} - \frac{i}{2}\Omega_p\rho_{32},\\
\dot\rho_{32} &= -\gamma_{32}\rho_{32} + \frac{i}{2}\Omega_c(\rho_{22} - \rho_{33}) - \frac{i}{2}\Omega_p^*\rho_{31} + \frac{i}{2}\Omega_s\rho_{12},\\
\dot\rho_{21} &= -(\gamma_{21} + i\delta_p)\rho_{21} + \frac{i}{2}\Omega_p(\rho_{11} - \rho_{22}) + \frac{i}{2}\Omega_c^*\rho_{31} - \frac{i}{2}\Omega_s\rho_{23},
\end{aligned} \tag{2}$$

where the damping rates γ_{31}, γ_{32} and γ_{21} are added phenomenologically.

We assume the weak-field approximation [4,65] and apply the perturbation $\rho_{ij} = \rho_{ij}^{(0)} + \rho_{ij}^{(1)} + ...$, where $\rho_{ij}^{(0)}, \rho_{ij}^{(1)}$, are of the zeroth and first order in the weak fields. We further assume that the quantum system is initially prepared in its ground level $|1\rangle$. In this case, the zeroth-order solution is $\rho_{00}^{(0)} \simeq 1$, and the other elements are zero ($\rho_{ij}^{(0)} = 0$).

Considering the steady state of the fields by neglecting the time derivatives in Eq. (2), and after some algebraic calculations, one can obtain the following off-diagonal density-matrix elements describing the corresponding first-order and second-order processes [64]:

$$\rho_{21}^{(1)} = \rho_{21}^{(L)} + \rho_{21}^{(N)} = \frac{i\Omega_p(\gamma_{31} + i\delta_p)}{2Y} + \frac{i^2\Omega_c^*\Omega_s}{4Y}, \tag{3a}$$

$$\rho_{31}^{(1)} = \rho_{31}^{(L)} + \rho_{21}^{(N)} = \frac{i\Omega_s(\gamma_{21} + i\delta_p)}{2Y} + \frac{i^2\Omega_p\Omega_c}{4Y}, \tag{3b}$$

with $Y = (\gamma_{21} + i\delta_p)(\gamma_{31} + i\delta_p) + |\Omega_c|^2/4$. The first terms $\rho_{21}^{(L)}$ and $\rho_{31}^{(L)}$ in Eqs. (3a) and (3b) are proportional with linear susceptibilities of the probe and sum-frequency generated signal beams. The second terms $\rho_{21}^{(N)}$ and $\rho_{31}^{(N)}$ describe the second-order nonlinear TWM and its backward nonlinear process via reabsorption, respectively [64]. Under the

slowly varying amplitude approximation, the Maxwell equations governing the propagation of the probe field and the generated sum-frequency signal field are

$$\frac{\partial \Omega_p}{\partial z} = i\alpha_{12}\rho_{21}^{(1)}, \tag{4a}$$

$$\frac{\partial \Omega_s}{\partial z} = i\alpha_{13}\rho_{31}^{(1)}, \tag{4b}$$

with the propagation constants $\alpha_{12}(\alpha_{13})$ proportional to $\omega_p|\mu_{12}|^2(\omega_p|\mu_{13}|^2)$. The diffraction terms containing the transverse derivatives $(2k_p)^{-1}\nabla_\perp^2\Omega_p$ and $(2k_s)^{-1}\nabla_\perp^2\Omega_s$ are disregarded in the Maxwell Eq. (4) ($k_p = \omega_p/c$ and $k_s = \omega_s/c$ are the central wave vectors of the probe and generated beams). These terms are considered as $\nabla_\perp^2\Omega_{p(s)} \sim \omega^{-2}\Omega_{p(s)}$, where ω is a characteristic transverse dimension of the laser beams. It can be a width of the vortex core if the beam carries an OAM or a characteristic width of the beam for a nonvortex beam. The change of the phase of the beams due to the diffraction term after passing the medium is then approximated to be $L/2k\omega^2$, where L is the length of the sample, with $k \approx k_{p(s)}$. The phase change $L/2k\omega^2$ can be neglected when the sample length is not too large, $L\lambda/\omega^2 \ll \pi$, where $\lambda = 2\pi/k$ is an optical wavelength. For instance, taking the length of the sample as $L = 100\,\mu$m, the characteristic transverse dimension of the beams to be $\omega = 20\,\mu$m, and the wavelength to be $\lambda = 1\,\mu$m, one finds $L\lambda/\omega^2 = 0.25$. The diffraction terms in such a condition do not play an important role and they can be neglected from Eq. (4).

Substituting Eq. (3) into the Maxwell Eqs. (4) results in

$$\frac{\partial \Omega_p}{\partial z} = i\alpha_{12}\left[\frac{i\Omega_p}{2Y}(\gamma_{31} + i\delta_p) + \frac{i^2\Omega_s\Omega_c^*}{4Y}\right], \tag{5a}$$

$$\frac{\partial \Omega_s}{\partial z} = i\alpha_{13}\left[\frac{i\Omega_s}{2Y}(\gamma_{21} + i\delta_p) + \frac{i^2\Omega_p\Omega_c}{4Y}\right]. \tag{5b}$$

III. EXCHANGE OF OPTICAL VORTICES

Let us consider a situation where the probe field is present at the entrance to the medium $\Omega_p(z=0) = \Omega_{p0}$ while the signal beam is absent $\Omega_s(z=0) = 0$. Assuming $\alpha_{12}\gamma_{31} = \alpha_{13}\gamma_{21}$ for simplicity, a solution to Eq. (5) for the generated signal light Ω_s reads

$$\Omega_s = \frac{\gamma_{21}}{\gamma_{31}}\Omega_{p0}\frac{\Omega_c}{\sqrt{\delta_p^2\left(1-\frac{\gamma_{21}}{\gamma_{31}}\right)^2 + |\Omega_c|^2\frac{\gamma_{21}}{\gamma_{31}}}}\sin\frac{\beta Z}{4Y} \times \exp\left[-\frac{\gamma_{31}Z}{2Y} - \frac{i\delta_p\left(1+\frac{\gamma_{31}}{\gamma_{21}}\right)Z}{4Y}\right], \tag{6}$$

where we have defined a modified propagation distance $Z = \alpha_{12}z$, and $\beta = \sqrt{\delta_p^2(1-\gamma_{31}/\gamma_{21})^2 + |\Omega_c|^2\gamma_{31}/\gamma_{21}}$. One can further simplify Eq. (6) for $\delta_p = 0$, leading to

$$\Omega_s = \sqrt{\frac{\gamma_{21}}{\gamma_{31}}}\Omega_{p0}\frac{\Omega_c}{|\Omega_c|}\exp \times\left[-\frac{\gamma_{31}}{\gamma_{21}\gamma_{31}+|\Omega_c|^2/4}Z\right]\sin\left(\frac{\sqrt{\gamma_{31}/\gamma_{21}}|\Omega_c|}{4\gamma_{21}\gamma_{31}+|\Omega_c|^2}Z\right). \tag{7}$$

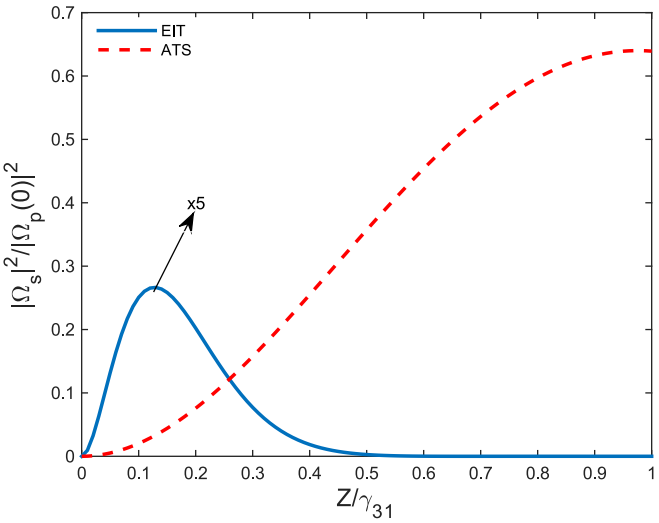

FIG. 2. The dependence of dimensionless intensity $|\Omega_s(z)|^2/|\Omega_p(0)|^2$ (TWM efficiency) against the effective propagation distance Z/γ_{31} in two different regimes of EIT ($|\Omega_c| = 0.3\gamma_{31}$) and ATS ($|\Omega_c| = 3\gamma_{31}$). The solid curve corresponds to the EIT regime and dashed curve corresponds to the ATS regime. The selected parameters are $\delta_p = 0$ and $\gamma_{21} = 0.05\gamma_{31}$.

Equations (6) and (7) indicate that the generated signal beam Ω_s can attain a vortex during its propagation if any of the probe Ω_p or the control Ω_c beams is initially a vortex. In this case, the OAM of initial vortices will be transferred to the generated signal Ω_s. The signal beam will have the same vorticity as the initial vortex beams. Such an optical vortex translation can be made possible in two different regimes; the EIT and the ATS. EIT occurs for the signal beam in the control field regime $|\Omega_c| < |\gamma_{31} - \gamma_{21}|$, while ATS appears in the control field regime $|\Omega_c| > |\gamma_{31} - \gamma_{21}|$ [8,64] (see also the discussion in the Appendix). This implies that tuning the knob of the control field causes smooth transition between the EIT and ATS. Assuming $\gamma_{21} = 0.05\gamma_{31}$, the EIT limit reduces to $|\Omega_c| < 0.95\gamma_{31}$ while it changes to $|\Omega_c| > 0.95\gamma_{31}$ for the ATS limit.

Before proceeding further, let us introduce the form of a beam carrying an optical vortex

$$\Omega_j = \varepsilon_j\left(\frac{r}{\omega}\right)^{|l_j|}e^{-\frac{r^2}{\omega^2}}e^{il_j\phi}, \tag{8}$$

with l_j, ϕ, ω, ε_j, and r parameters denoting OAM number, the azimuthal angle, the beam waist, the strength of the beam, and a cylindrical radius.

A. OAM exchange from probe to signal

With the goal of efficient transfer of optical vortices, let us first consider a situation where the probe beam Ω_p is vortex defined by Eq. (8) with $j = p$. Figure 2 shows the dependence of dimensionless intensity $|\Omega_s(z)|^2/|\Omega_p(0)|^2$ against the effective propagation distance in two different regimes of EIT [$|\Omega_c| = 0.3\gamma_{31}$(a)] and ATS [$|\Omega_c| = 3\gamma_{31}$ (b)]. From Fig. 2(a), one can see that when $\delta_p = 0$, the generated beam in the EIT limit is completely suppressed by the unwanted absorption effects that cause signal loss on propagation, eliminating the

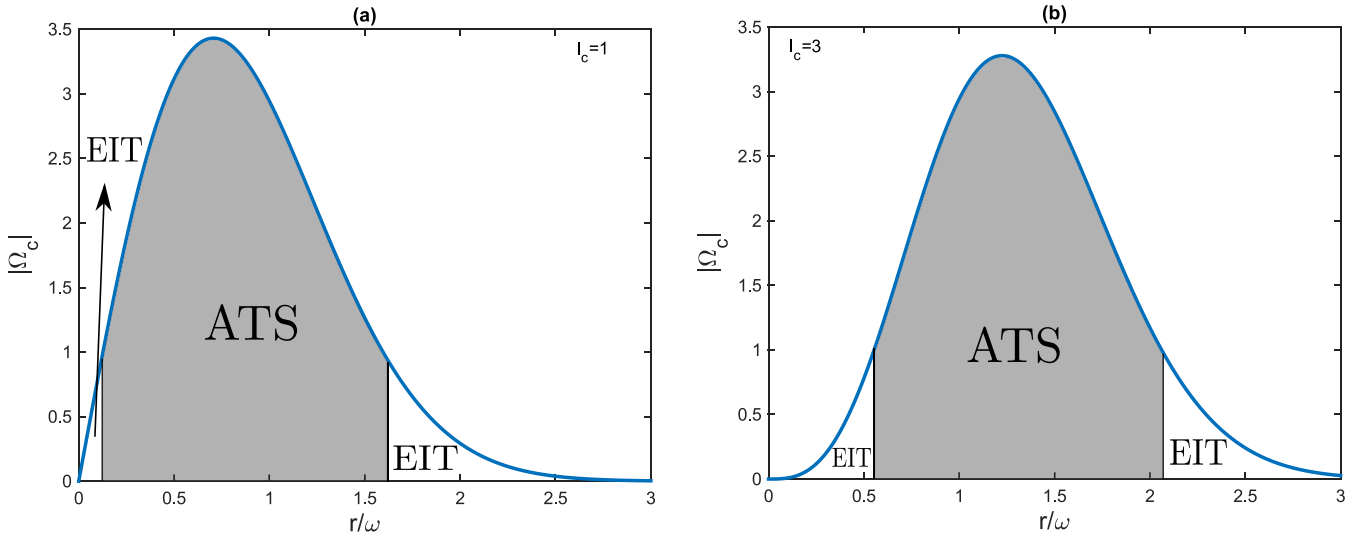

FIG. 3. Intensity of control field $|\Omega_c|$ as a function of r/ω for (a) $l_c = 1$ and (b) $l_c = 3$. The selected parameter is $\varepsilon_c = 8\gamma_{31}$.

TWM efficiency for larger propagating distances. On the other hand, the vortex conversion efficiency is enhanced by the ATS. The maximum conversion efficiency in this case is observed to reach 60%. This implies that the energy conversion between probe and signal beams carrying an OAM in the ATS condition is considerably more efficient than that in the EIT limit.

B. OAM exchange from control to signal

In a second OAM exchange scenario, we consider a situation where the strong coupling field Ω_c is an optical vortex defined by Eq. (8) with $j = c$. As the control field is now inhomogeneous, we need to identify the limits for the ATS and EIT regimes. The intensity of control field $|\Omega_c|$ is plotted in Fig. 3 versus r/ω when $\varepsilon_c = 8\gamma_{31}$ and for different OAM numbers $l_c = 1$ (a) and $l_c = 3$ (b), respectively. The white area represents the cylindrical radius zone where the EIT is dominant ($|\Omega_c| < 0.95\gamma_{31}$), while the gray area shows the ATS zone ($|\Omega_c| > 0.95\gamma_{31}$). Larger OAM numbers shift the beam intensity profile; therefore, the EIT and ATS will be established at different radial distance.

Identifying the cylindrical radius limits for the EIT and ATS, we demonstrate in Fig. 4 the efficiency of TWM versus r/ω for (a) $l_c = 1$ and (b) $l_c = 3$ at $\delta_p = 0$. As expected, the mixing efficiency in the EIT regime is quite lower than that in the ATS regime. Moreover, the efficiency of TWM is changed over the radial zone when the topological charge of vortex beam is varied.

As shown in Fig. 4, the system lies always in the ATS regime at $r/\omega = 1.4$, while it goes to the EIT regime at $r/\omega = 2.5$. The effect of OAM number l_c on the efficiency of TWM in both the ATS (a) and EIT (b) regimes is illustrated in Fig. 5. One can see that the maximum TWM vortex conversion efficiency for the EIT is quite low even for larger OAM numbers,

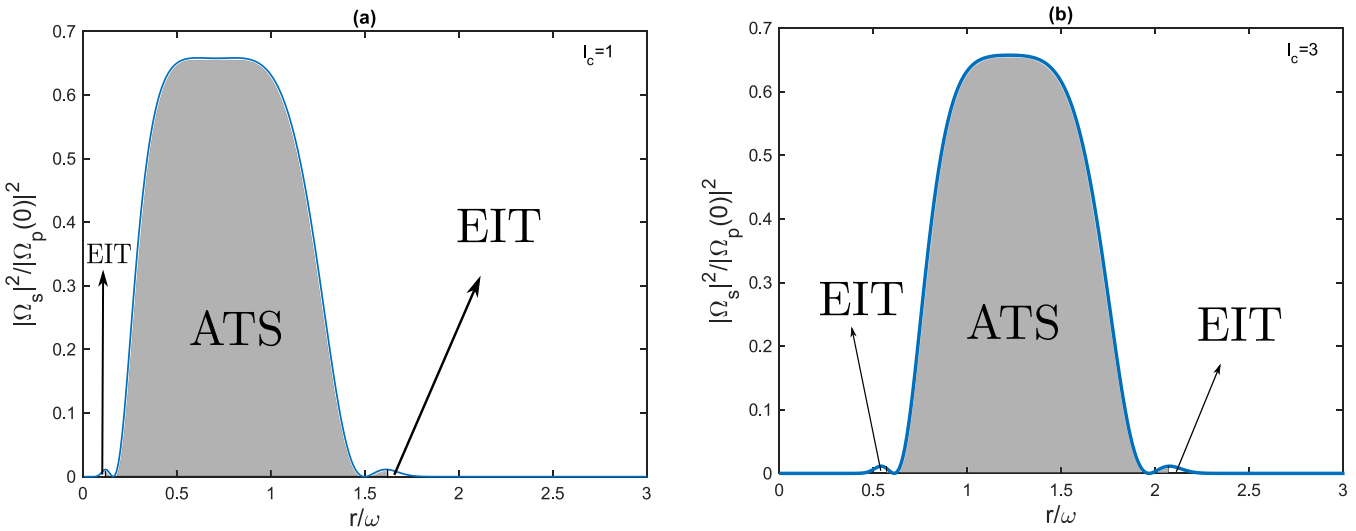

FIG. 4. TWM efficiency as a function of r/ω for (a) $l_c = 1$ and (b) $l_c = 3$. The selected parameters are $\gamma_{21} = 0.05\gamma_{31}$, $\delta_p = 0$, $\varepsilon_c = 8\gamma_{31}$, and $Z = 1\gamma_{31}$.

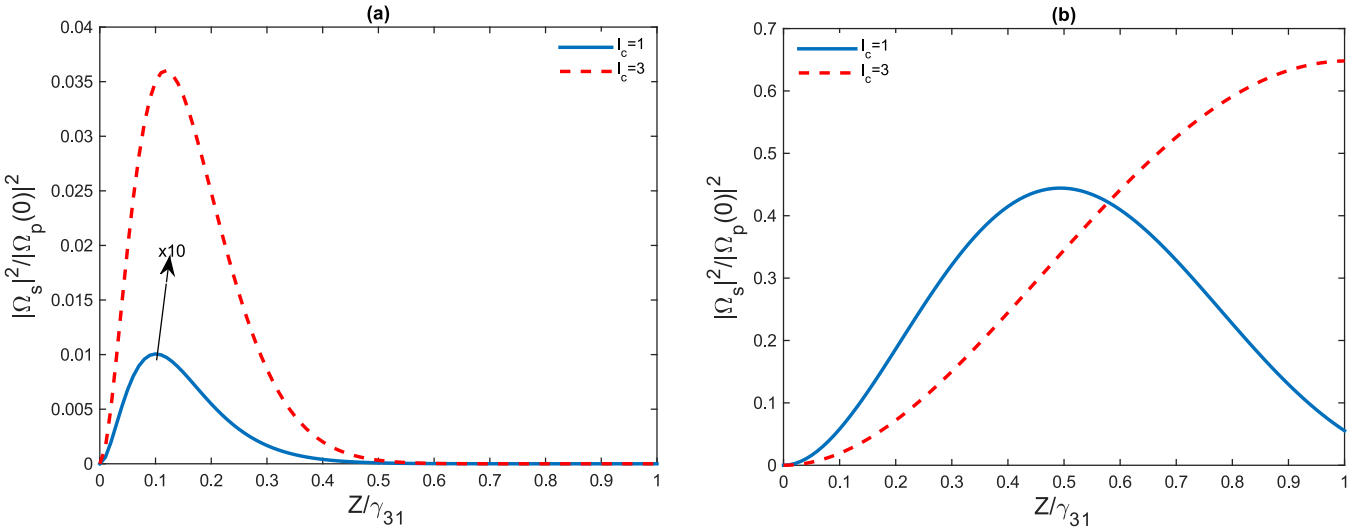

FIG. 5. TWM efficiency against the effective propagation distance Z/γ_{31} in (a) EIT regime ($r/\omega = 2.5$), and (b) ATS regime ($r/\omega = 1.4$). The selected parameters are $\gamma_{21} = 0.05\gamma_{31}$, $\delta_p = 0$, and $\varepsilon_c = 8\gamma_{31}$. The solid (dashed) curve corresponds to the OAM number $l_c = 1$ ($l_c = 3$).

and vanishes on propagation [see Fig. 5(a)]. However, the conversion efficiency becomes considerably large in the ATS limit, while it is enhanced for larger OAM numbers [see the dashed curve in Fig. 5(b) for $l_c = 3$].

To get a deeper physical insight into the origin of above results, we plot in Fig. 6 the dependence of dimensionless intensity $|\Omega_s(z)|^2/|\Omega_p(0)|^2$ against the probe field detuning δ_p. We select $r/\omega = 2.5$ in Fig. 6(a) to satisfy the EIT limit ($|\Omega_c| < 0.95\gamma_{31}$) on resonance of the probe field, while $r/\omega = 1.4$ in Fig. 6(b) for the ATS limit ($|\Omega_c| > 0.95\gamma_{31}$) at $\delta_p = 0$. Obviously, there is a hole bored into the TWM efficiency profile [Fig. 6(a)]. This suggests the presence of strong absorption losses in the EIT limit when $|\Omega_c| < 0.95\gamma_{31}$, which suppresses the nonlinear sum-frequency process and reduces the efficiency of vortex conversion on resonance. The resonant TWM efficiency is greatly enhanced for the ATS case when $|\Omega_c| > 0.95\gamma_{31}$, indicating the superiority of ATS to significantly enhance the nonlinear sum-frequency vortex generation.

IV. SUMMARY

In summary, we have considered propagation of optical vortices in a symmetry-broken three-level ladder quantum coupling scheme interacting with probe, signal and control beams. We studied the light-matter interaction under the situation where either the control or the probe beams carries optical vortices. We have shown that the OAM of the initial vortex beams can be transferred to a generated signal field via a TWM process, and under two different regimes of EIT and ATS. It is shown that the ATS regime provides much more powerful condition than the EIT to exchange optical vortices with maximum efficiency.

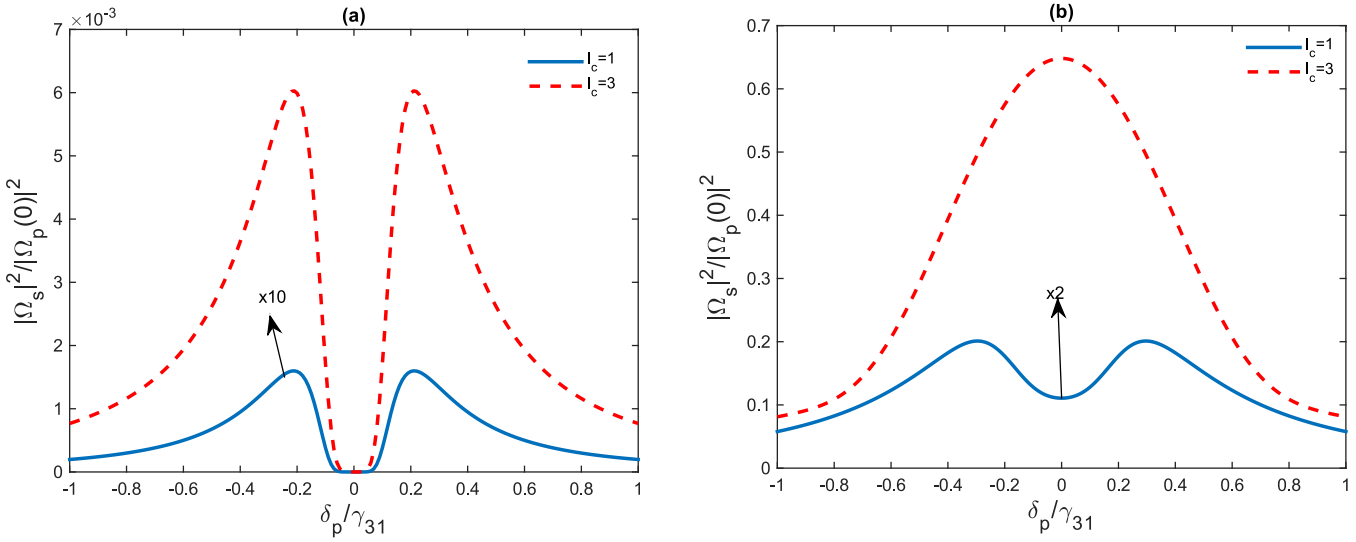

FIG. 6. TWM efficiency against the probe field detuning δ_p for (a) $r/\omega = 2.5$, and (b) $r/\omega = 1.4$. Here, $Z = 1\gamma_{31}$, and the other selected parameters are same as Fig. 5. The solid (dashed) curve corresponds to the OAM number $l_c = 1$ ($l_c = 3$).

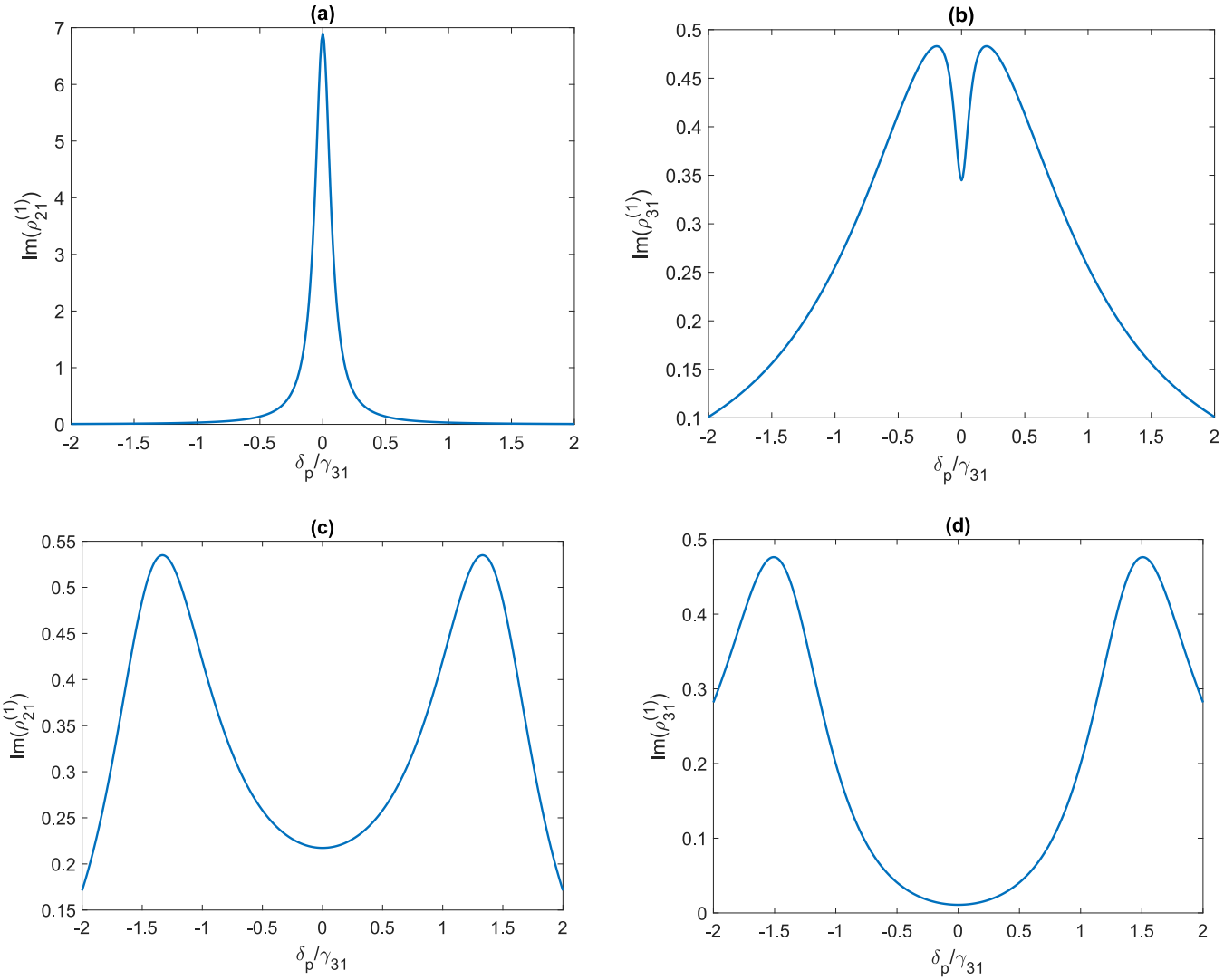

FIG. 7. The absorption spectrum of the system for the probe (a),(c) and signal (b),(d) beams against the probe field detuning δ_p for $\Omega_c = 0.3\gamma_{31}$(a),(b) and $\Omega_c = 3\gamma_{31}$(c),(d). The selected parameters are same as Fig. 2.

A threshold factor $|\gamma_{31} - \gamma_{21}|$ is introduced to distinguish between two different regimes where the OAM exchange can occur. An increase of the intensity of the control field results in a transition from EIT to ATS. EIT (ATS) is established when the absolute value of the control field Rabi frequency is smaller (larger) than the threshold factor. This indicates that in the pursuit of empirically optimized high efficiency OAM exchange process, the spatial shape of an intense control beam becomes important if this beam carries an OAM. However, the spatial profile of the weak probe field does not play any impact in efficiency of energy conversion as the threshold factor is controlled only by Ω_c.

It should be pointed out that in addition to the two cases proposed here for the exchange of vortices (probe to signal and control to signal), the OAM exchange can take place under the condition where both probe and control fields are initially vortices. The generated vortex beam in this case acquires a vorticity of $l_c + l_p$. Yet, the generated beam will experience strong absorption losses at the vortex core.

APPENDIX: EIT AND ATS FOR THE PROBE AND SIGNAL BEAMS

In this Appendix we make a few remarks related to the three-level scheme proposed here and discuss conditions for the appearance of EIT and ATS for the probe and signal beams, enabling us to elucidate the origin of higher OAM conversion in the ATS regime. We do so by studying absorption dependence of probe and signal beams without taking into account any transverse dependence of the applied fields. The light-matter coupling scheme illustrated in Fig. 1 can be viewed as a three-level ladder-type EIT system with an additional signal beam Ω_s, making a closed-loop level structure. Such a closed-loop light-matter coupling consists of two subschemes: (i) a ladder-type scheme which is composed of $|1\rangle \overset{\Omega_p}{\rightarrow} |2\rangle$ and $|2\rangle \overset{\Omega_c}{\rightarrow} |3\rangle$ transitions, and (ii) a Λ-type scheme made of transitions $|1\rangle \overset{\Omega_s}{\rightarrow} |3\rangle$ and $|3\rangle \overset{\Omega_c}{\rightarrow} |2\rangle$.

Let us now consider the decay rates γ_{31}, γ_{21}. In this paper all involving parameters have been scaled by γ_{31}, while

we have assumed $\gamma_{31} \gg \gamma_{21}$ such that a threshold factor $|\gamma_{31} - \gamma_{21}|$ distinguishes the EIT and ATS limits. This assumption for the decay rates makes it impossible to observe EIT in the ladder scheme (i) when $|\Omega_c| \ll \gamma_{31}$. Note that for the ladder scheme (i) state $|3\rangle$ plays the role of a metastable state which should weakly decay to get a perfect EIT $\gamma_{31} \to 0$, or $|\Omega_c| \gg \gamma_{31}$ in order to observe an imperfect EIT. Therefore, we expect a strong resonant absorption (instead of EIT) for the weak probe field in the ladder scheme (i) in the regime $|\Omega_c| \ll \gamma_{31}$, as can be seen in Fig. 7(a).

On the other hand for the Λ scheme (ii) the middle state $|3\rangle$ strongly decays, while the metastable state $|2\rangle$ decays with a very weak rate. Therefore, the resonant absorption effects can be reduced even for the weak coupling fields $|\Omega_c| \ll \gamma_{31}$ [see Fig. 7(b)], which is the feature of EIT. Figure 7(d) shows that stronger coupling intensities results in a more pronounced transparency window around zero detuning due to the ATS effect. Therefore, one may distinguish the EIT and ATS by the coupling field intensity for the behavior of the signal field [in the Λ scheme (ii)]. This is not, however, possible for the behavior of the probe field [ladder scheme (i)], as no EIT happens for a weak coupling field, and one may only see absorption reduction in the probe field by a strong coupling field and due to the ATS [see Fig. 7(c)]. This discussion explicitly demonstrates the reason for superiority of ATS over EIT in more efficient exchange of optical vortices as the probe field in the EIT case always experiences absorption losses at $\delta_p = 0$.

[1] S. E. Harris, J. E. Field, and A. Imamoğlu, Nonlinear Optical Processes using Electromagnetically Induced Transparency, Phys. Rev. Lett. **64**, 1107 (1990).

[2] S. E. Harris, Electromagnetically induced transparency, Phys. Today **50**(7), 36 (1997).

[3] M. D. Lukin, Colloquium: Trapping and manipulating photon states in atomic ensembles, Rev. Mod. Phys. **75**, 457 (2003).

[4] M. Fleischhauer, A. Imamoglu, and J. P. Marangos, Electromagnetically induced transparency: Optics in coherent media, Rev. Mod. Phys. **77**, 633 (2005).

[5] Y. Wu, J. Saldana, and Y.-F. Zhu, Large enhancement of four-wave mixing by suppression of photon absorption from electromagnetically induced transparency, Phys. Rev. A **67**, 013811 (2003).

[6] X.-X. Yang, Z.-W. Li, and Y. Wu, Four-wave mixing via electron spin coherence in a quantum well waveguide, Phys. Lett. A **340**, 320 (2005).

[7] Y. Wu and X.-X. Yang, Highly efficient four-wave mixing in double lambda system in ultraslow propagation regime, Phys. Rev. A **70**, 053818 (2004).

[8] H.-C. Li, G.-Q. Ge, and M. S. Zubairy, High-efficiency four-wave mixing beyond pure electromagnetically induced transparency treatment, Opt. Lett. **44**, 3486 (2019).

[9] M. O. Scully, From lasers and masers to phaseonium and phasers, Phys. Rep. **219**, 191 (1992).

[10] L. Hau, S. Harris, Z. Dutton, and C. Behroozi, Light speed reduction to 17 metres per second in an ultracold atomic gas, Nature (London) **397**, 594 (1999).

[11] L. J. Wang, A. Kuzmich, and A. Dogariu, Gain-assisted superluminal light propagation, Nature (London) **406**, 277 (2000).

[12] D. F. Phillips, A. Fleischhauer, A. Mair, R. L. Walsworth, and M. D.Lukin, Storage of Light in Atomic Vapor, Phys. Rev. Lett. **86**, 783 (2001).

[13] C. Liu, Z. Dutton, C. Behroozi, and L. V. Hau, Observation of coherent optical information storage in an atomic medium using halted light pulses, Nature (London) **409**, 490 (2001).

[14] M. O. Scully, Enhancement of the Index of Refraction Via Quantum Coherence, Phys. Rev. Lett. **67**, 1855 (1991).

[15] J. B. Pendry, Negative Refraction Makes a Perfect Lens, Phys. Rev. Lett. **85**, 3966 (2000).

[16] Ying Wu, Two-color ultraslow optical solitons via four-wave mixing in cold-atom media, Phys. Rev. A **71**, 053820 (2005).

[17] Y. Wu and L. Deng, Ultraslow Optical Solitons in a Cold Four-State Medium, Phys. Rev. Lett. **93**, 143904 (2004).

[18] Y. Chen, Z.-Y. Bai, and G.-X. Huang, Ultraslow optical solitons and their storage and retrieval in an ultracold ladder-type atomic system, Phys. Rev. A **89**, 023835 (2014).

[19] Y.-P. Niu and S.-Q. Gong, Enhancing Kerr nonlinearity via spontaneously generated coherence, Phys. Rev. A **73**, 053811 (2006).

[20] H. R. Hamedi and G. Juzeliūnas, Phase-sensitive Kerr nonlinearity for closed-loop quantum systems, Phys. Rev. A **91**, 053823 (2015).

[21] H. Schmidt and A. Imamoglu, Giant Kerr nonlinearities obtained by electromagnetically induced transparency, Opt. Lett. **21**, 1936 (1996).

[22] S. H. Autler and C. H. Townes, Stark effect in rapidly varying fields, Phys. Rev. **100**, 703 (1955).

[23] R. Shimano and M. Kuwata-Gonokami, Observation of Autler-Townes Splitting of Biexcitons in CuCl, Phys. Rev. Lett. **72**, 530 (1994).

[24] T. Y. Abi-Salloum, Electromagnetically induced transparency and Autler-Townes splitting: Two similar but distinct phenomena in two categories of three-level atomic systems, Phys. Rev. A **81**, 053836 (2010).

[25] L.-Y. He, T.-J. Wang, Y.-P. Gao, C. Cao, and C. Wang, Discerning electromagnetically induced transparency from Autler-Townes splitting in plasmonic waveguide and coupled resonators system, Opt. Express **23**, 23817 (2015).

[26] P. M. Anisimov, J. P. Dowling, and B. C. Sanders, Objectively Discerning Autler-Townes Splitting from Electromagnetically Induced Transparency, Phys. Rev. Lett. **107**, 163604 (2011).

[27] L. Giner *et al.*, Experimental investigation of the transition between Autler-Townes splitting and electromagnetically-induced-transparency models, Phys. Rev. A **87**, 013823 (2013).

[28] C. Tan and G. Huang, Crossover from electromagnetically induced transparency to Autler-Townes splitting in open ladder systems with Doppler broadening, J. Opt. Soc. Am. B **31**, 704 (2014).

[29] H.-C. Sun, Y.-x. Liu, H. Ian, J. Q. You, E. Il'ichev, and F. Nori, Electromagnetically induced transparency and Autler-Townes splitting in superconducting flux quantum circuits, Phys. Rev. A **89**, 063822 (2014).

[30] X. Lu, X. Miao, J. Bai, L. Pei, M. Wang, Y. Gao, L.-A. Wu, P. Fu, R. Wang, and Z. Zuo, Transition from Autler–Townes splitting to electromagnetically induced transparency based on the dynamics of decaying dressed states, J. Phys. B **48**, 055003 (2015).

[31] L. Hao, Y. Jiao, Y. Xue, X. Han, S. Bai, J. Zhao, and G. Raithel, Transition from electromagnetically induced transparency to Autler–Townes splitting in cold cesium atoms, New J. Phys. **20**, 073024 (2018).

[32] A. Rastogi, E. Saglamyurek, T. Hrushevskyi, S. Hubele, and L. J. LeBlanc, Discerning quantum memories based on electromagnetically-induced-transparency and Autler-Townes-splitting protocols, Phys. Rev. A **100**, 012314 (2019).

[33] L. Allen, M. J. Padgett, and M. Babiker, IV The Orbital Angular Momentum of Light, Prog. Opt. **39**, 291 (1999).

[34] L. Allen, S. M. Barnett, and M. J. Padgett, *Optical Angular Momentum* (Bristol, UK, 2003).

[35] N. R. Heckenberg, R. McDuff, C. P. Smith, and A. G. White, Generation of optical phase singularities by computer-generated holograms, Opt. Lett. **17**, 221 (1992).

[36] I. G. Mariyenko, J. Strohaber, and C. J. G. J. Uiterwaal, Creation of optical vortices in femtosecond pulses, Opt. Express **13**, 7599 (2005).

[37] N. Jia, J. Qian, T. Kirova, G. Juzeliūnas, and H. R. Hamedi, Ultraprecise Rydberg atomic localization using optical vortices, Opt. Express **28**, 36936 (2020).

[38] Q.-F. Chen, B.-S. Shi, Y.-S. Zhang, and G.-C. Guo, Entanglement of the orbital angular momentum states of the photon pairs generated in a hot atomic ensemble, Phys. Rev. A **78**, 053810 (2008).

[39] V. E. Lembessis, D. Ellinas, M. Babiker, and O. Al-Dossary, Atom vortex beams, Phys. Rev. A **89**, 053616 (2014).

[40] M. F. Andersen, C. Ryu, P. Cladé, V. Natarajan, A. Vaziri, K. Helmerson, and W. D. Phillips, Quantized Rotation of Atoms From Photons with Orbital Angular Momentum, Phys. Rev. Lett. **97**, 170406 (2006).

[41] M. Babiker, W. L. Power, and L. Allen, Light-Induced Torque on Moving Atoms, Phys. Rev. Lett. **73**, 1239 (1994).

[42] V. E. Lembessis and M. Babiker, Light-induced torque for the generation of persistent current flow in atomic gas Bose-Einstein condensates, Phys. Rev. A **82**, 051402(R) (2010).

[43] N. Radwell, T. W. Clark, B. Piccirillo, S. M. Barnett, and S. Franke-Arnold, Spatially Dependent Electromagnetically Induced Transparency, Phys. Rev. Lett. **114**, 123603 (2015).

[44] H. R. Hamedi, V. Kudriasov, J. Ruseckas, and G. Juzeliūnas, Azimuthal modulation of electromagnetically induced transparency using structured light, Opt. Express **26**, 28249 (2018).

[45] G. Walker, A. S. Arnold, and S. Franke-Arnold, Trans-Spectral Orbital Angular Momentum Transfer Via Four-Wave Mixing in Rb Vapor, Phys. Rev. Lett. **108**, 243601 (2012).

[46] J. Dalibard, F. Gerbier, G. Juzeliūnas, and P. Öhberg, Colloquium: Artificial gauge potentials for neutral atoms, Rev. Mod. Phys. **83**, 1523 (2011).

[47] J. Ruseckas, V. Kudriašov, I. A. Yu, and G. Juzeliūnas, Transfer of orbital angular momentum of light using two-component slow light, Phys. Rev. A **87**, 053840 (2013).

[48] H. R. Hamedi, J. Ruseckas, and G. Juzeliūnas, Exchange of optical vortices using an electromagnetically-induced-transparency-based four-wave-mixing setup, Phys. Rev. A **98**, 013840 (2018).

[49] H. R. Hamedi, E. Paspalakis, G. Žlabys, G. Juzeliūnas, and J. Ruseckas, Complete energy conversion between light beams carrying orbital angular momentum using coherent population trapping for a coherently driven double-Λ atom-light-coupling scheme, Phys. Rev. A **100**, 023811 (2019).

[50] H. R. Hamedi, J. Ruseckas, E. Paspalakis, and G. Juzeliūnas, Transfer of optical vortices in coherently prepared media, Phys. Rev. A **99**, 033812 (2019).

[51] M. Mahdavi, Z. A. Sabegh, M. Mohammadi, M. Mahmoudi, and H. R. Hamedi, Manipulation and exchange of light with orbital angular momentum in quantum-dot molecules, Phys. Rev. A **101**, 063811 (2020).

[52] Rahmatullah, M. Abbas, Ziauddin, and S. Qamar, Spatially structured transparency and transfer of optical vortices via four-wave mixing in a quantum-dot nanostructure, Phys. Rev. A **101**, 023821 (2020).

[53] Y.-F. Zhang, Z.-P. Wang, J. Qiu, Y. Hong, and B. Yu, Spatially dependent four-wave mixing in semiconductor quantum wells, Appl. Phys. Lett. **115**, 171905 (2019).

[54] J. Qiu, Z.-P. Wang, D.-S. Ding, W. B. Li, and B. Yu, Highly efficient vortex four-wave mixing in asymmetric semiconductor quantum wells, Opt. Express **28**, 2975 (2020).

[55] Z.-P. Wang, Y.-F. Zhang, E. Paspalakis, and B. Yu, Efficient spatiotemporal-vortex four-wave mixing in a semiconductor nanostructure, Phys. Rev. A **102**, 063509 (2020).

[56] S. Wielandy and A. L. Gaeta, Investigation of electromagnetically induced transparency in the strong probe regime, Phys. Rev. A **58**, 2500 (1998).

[57] M. A. Sillanpää, J. Li, K. Cicak, F. Altomare, J. I. Park, R. W. Simmonds, G. S. Paraoanu, and P. J. Hakonen, Autler-Townes Effect in a Superconducting Three-Level System, Phys. Rev. Lett. **103**, 193601 (2009).

[58] P. Král, I. Thanopulos, M. Shapiro, and D. Cohen, Two-Step Enantio-Selective Optical Switch, Phys. Rev. Lett. **90**, 033001 (2003).

[59] Y. X. Liu, J. Q. You, L. F. Wei, C. P. Sun, and F. Nori, Optical Selection Rules and Phase-Dependent Adiabatic State Control in a Superconducting Quantum Circuit, Phys. Rev. Lett. **95**, 087001 (2005).

[60] P. Král, I. Thanopulos, and M Shapiro, Colloquium: Coherently controlled adiabatic passage, Rev. Mod. Phys. **79**, 53 (2007).

[61] V. E. Manucharyan, J. Koch, L. I. Glazman, and M. H. Devoret, Fluxonium: Single cooper-pair circuit free of charge offsets, Science **326**, 113 (2009).

[62] V. E. Manucharyan, N. A. Masluk, A. Kamal, J. Koch, L. I. Glazman, and M. H. Devoret, Evidence for coherent quantum phase slips across a Josephson junction array, Phys. Rev. B **85**, 024521 (2012).

[63] L. Zhou, L. P. Yang, Y. Li, and C. P. Sun, Quantum Routing of Single Photons with a Cyclic Three-Level System, Phys. Rev. Lett. **111**, 103604 (2013).

[64] H.-C. Li, G.-Q. Ge, and M. S. Zubairy, Efficient nonlinear frequency mixing using Autler-Townes splitting, Phys. Rev. A **102**, 053701 (2020).

[65] M. O. Scully and M. S. Zubairy, *Quantum Optics* (Cambridge University Press, Cambridge, 1997).